HYSTERETIC ENDOCHRONIC THEORY FOR SAND

By Zdeněk P. Bažant,[1] Raymond J. Krizek,[2] and Chin-Long Shieh,[3] Members ASCE

ABSTRACT: A new form of endochronic constitutive model is presented to describe the behavior of dry or drained sand, and its parameters are determined by extensive comparisons with published test data. Jump-kinematic hardening is used to guarantee that the hysteresis loops always close, yield positive energy dissipation, and give an increase in tangent modulus when unloading changes to reloading. Criteria for virgin loading, unloading and reloading are formulated in terms of deviatoric work, and changes of material parameters at loading-unloading-reloading transition points are determined. Two endochronic units coupled in parallel are used to describe the measured response over a broad range of strain amplitude. The inelastic volume change is characterized so as to include both densification and dilatancy. Certain material properties are determined as functions of the void ratio. Calculations show that the lateral stress in a simple shear test quickly becomes almost equal to the vertical stress. A three-dimensional finite element analysis of the simple shear test with endochronic theory reveals significant stress nonuniformity; but this is found to have little effect on the resulting hysteresis loops.

INTRODUCTION

Endochronic theory provides an effective model for describing the mechanical behavior of materials in which the inelastic strain develops gradually, and previous applications to metals (29), concrete (8), and sand (10,14) has met with considerable success. However, these early models were unable to properly characterize the response to small cyclic stress oscillations superimposed on large static stresses. For this case the original theory does not give positive energy dissipation or closed hysteresis loops, and it yields a reloading slope that is less steep than the unloading slope. Recently it has been found (4) that these features can be corrected at the expense of introducing loading-unloading-reloading criteria and the so-called jump-kinematic hardening.

The objective of this paper, which is based on a 1979 report (11), is to develop for sand a constitutive relation which describes well the hysteretic aspects for arbitrarily variable stress or strain and is based on the jump-kinematic hardening concept. This approach parallels a similar development for concrete (12) in which the jump-kinematic hardening has also been used, although in a very different constitutive relation. Compared to previous applications of endochronic theory to soils, the present model will also involve various further refinements, such as the inclusion of inelastic dilatancy and the use of two endochronic units coupled in parallel, and determination of the dependence of material parameters

[1]Prof. of Civ. Engrg. and Dir., Center for Concrete and Geomaterials, Northwestern University, Evanston, Ill. 60201.

[2]Prof. and Chmn., Dept. of Civ. Engrg., Northwestern University, Evanston, Ill. 60201.

[3]Sr. Struct. Engrg. Specialist, Sargent and Lundy Engineers, Chicago, Ill.

Note.—Discussion open until January 1, 1984. To extend the closing date one month, a written request must be filed with the ASCE Manager of Technical and Professional Publications. The manuscript for this paper was submitted for review and possible publication on July 2, 1981. This paper is part of the Journal of Engineering Mechanics, Vol. 109, No. 4, August, 1983. ©ASCE, ISSN 0733-9399/83/0004-1073/$01.00. Paper No. 18150.

on the void ratio. These will make it possible to model the response in simple shear tests and in triaxial tests with one and the same constitutive relation. Finally, three-dimensional finite elements will be used to estimate the stress nonuniformity in the specimen and its effect on hysteresis loops. It should be also noted that various other developments in endochronic modeling of geomaterials have been made recently (1, 2, 6, 7, 13, 17, 18, 25, Wu, H.-C., "Endochronic Theory for the Mechanical Behavior of Cohesionless Soil Under Static Loading," *Journal of Engineering Mechanics Division*, ASCE, (in press)). Useful criticisms of certain aspects of endochronic theory have been raised by Sandler (23) and Rivlin (22), and revisions to eliminate the criticized aspects were proposed, e.g., in Refs. 4 and 5.

Endochronic Loading Surfaces

Although endochronic theory was originally developed without the concept of a loading surface (29), it is helpful to introduce this concept as a logical way to formulate kinematic hardening. We may begin by considering deviatoric deformations which are modeled by two viscoplastic Maxwell units coupled in parallel (Fig. 1(*a*)):

$$s_{ij} = s_{ij}^{(1)} + s_{ij}^{(2)} \quad \ldots\ldots (1)$$

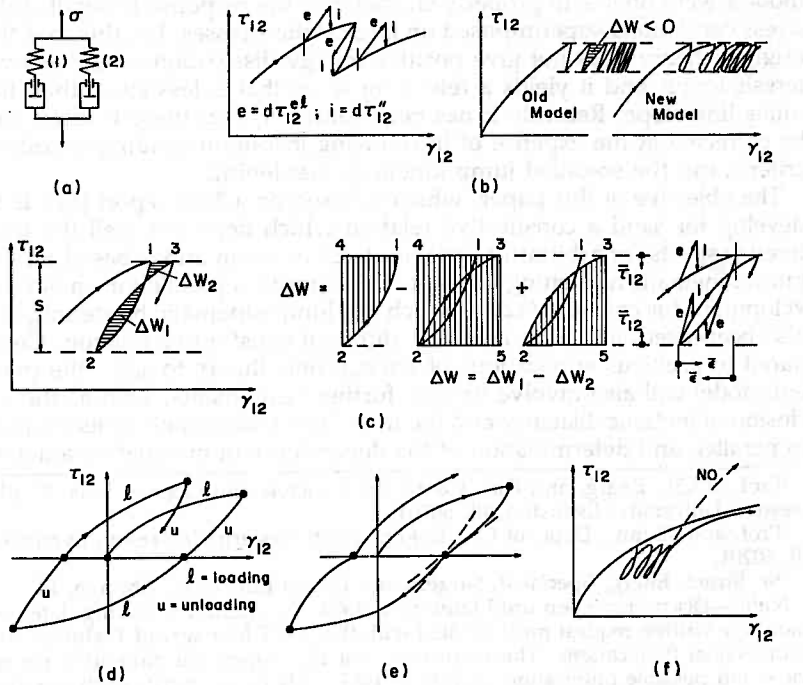

FIG. 1.—Explanatory Diagrams on Hysteresis

$$ds_{ij}^{(1)} = 2G_1 de_{ij} - \frac{\partial \Phi_1}{\partial s_{ij}} \frac{d\zeta}{Z_1}; \quad ds_{ij}^{(2)} = 2G_2 de_{ij} - \frac{\partial \Phi_2}{\partial s_{ij}} \frac{d\zeta}{Z_2} \quad \ldots\ldots (2)$$

in which $e_{ij} = \epsilon_{ij} - \delta_{ij}\epsilon$ = strain deviator; $s_{ij} = \sigma_{ij} - \delta_{ij}\sigma$ = stress deviator; δ_{ij} = Kronecker delta; ϵ_{ij} = components of the small strain tensor, $\boldsymbol{\epsilon}$; and σ_{ij} = components of the stress tensor, $\boldsymbol{\sigma}$. Subscripts i and j refer to cartesian coordinates x_i (i = 1, 2, 3), and superscripts 1 and 2 in parentheses denote the number of the unit in the chain model (Fig. 1(*a*)). G_1 and G_2 are the corresponding shear moduli; Z_1 and Z_2 are the corresponding rate coefficients; Φ_1 and Φ_2 are functions of σ_{ij} which define the corresponding loading surfaces; ζ is a parameter known as intrinsic time, introduced by Valanis (29) together with the term endochronic theory.

Classical viscoplasticity uses a parameter similar to ζ in Eq. 2, namely the reduced time $\zeta = \int dt/a_D$, where t is time and a_D is a time shift factor that can depend on σ_{ij} and ϵ_{ij}. Schapery (24) introduced a new idea—the dependence of a_D on the strain rate, $\dot{\epsilon}_{ij}$, where the dot refers to a time derivative. In particular, he proposed that $1/a_D$ should depend on the octahedral shear component of ϵ_{ij}, i.e., on $\bar{e} = (\dot{e}_{km}\dot{e}_{km}/2)^{1/2}$. Introducing a linear dependence $1/a_D = cF\bar{e}$ with proportionality factors cF yields $d\zeta = cF\bar{e}dt$, which may be rewritten as

$$d\zeta = cF(\boldsymbol{\sigma}, \boldsymbol{\epsilon}, \xi)d\xi; \quad d\xi = \sqrt{\frac{1}{2} de_{km} de_{km}} \quad \ldots\ldots (3)$$

(repeated subscripts imply summation over 1, 2, 3). Note that ξ is independent of time and actually represents the path length in deviatoric strain space. The assumption of $d\zeta = (cF\bar{e} + \text{constant})\,dt$ would render the theory time dependent, but time effects will not be considered here.

Valanis (29) developed the thermodynamic framework of this theory and was the first to realize that the above definition of $d\xi$ is useful for modeling gradual development of inelastic strain at unloading and cyclic loading. The endochronic theory proposed for metals by Valanis (29), as well as that initially developed for sand (10,14) may be shown to correspond to a loading function which exhibits isotropic hardening and has a von Mises type deviatoric term, i.e., $\Phi = s_{km}s_{km} - H_1$, where H_1 is a parameter. However, in case of cyclic loading the corresponding constitutive equation was later found to exhibit certain objectionable features with regard to energy dissipation during hysteretic loops. A method to eliminate these by means of a certain novel type of kinematic hardening has been proposed in general terms in previous works (3,4).

In all kinematic hardening rules the center of the yield surface does not remain at the origin, but moves. Accordingly, assuming the loading surfaces to be of von Mises type, we may set

$$\Phi_1 = \frac{1}{2}(s_{km}^{(1)} - \alpha_{km}^{(1)})(s_{km}^{(1)} - \alpha_{km}^{(1)}) - H_1;$$

$$\Phi_2 = \frac{1}{2}(s_{km}^{(2)} - \alpha_{km}^{(2)})(s_{km}^{(2)} - \alpha_{km}^{(2)}) - H_2 \quad \ldots\ldots (4)$$

in which $\alpha_{km}^{(1)}$ and $\alpha_{km}^{(2)}$ are the current centers of the deviatoric loading surfaces, and Φ_1 and Φ_2 and H_1 and H_2 are parameters which have no

effect on the constitutive relation. Substituting Eq. 4 into Eq. 1, the deviatoric stress-strain relations become

$$ds_{ij}^{(1)} = 2G_1 de_{ij} - (s_{ij}^{(1)} - \alpha_{ij}^{(1)}) \frac{d\zeta}{Z_1}; \quad ds_{ij}^{(2)} = 2G_2 de_{ij} - (s_{ij}^{(2)} - \alpha_{ij}^{(2)}) \frac{d\zeta}{Z_2} \quad \ldots\ldots (5)$$

Although a model consisting of several parallel endochronic Maxwell units was considered in the preceding studies (10), the test data were fitted with a single unit model. The reason for considering two parallel units instead of one is to achieve a good representation of hysteretic loops for both small and large strain magnitudes. As the strain increases, there is a large decrease in the tangent modulus of sands (in contrast to concrete), and one endochronic unit (which suffices for concrete) is inadequate to properly model this decrease. In fact, the use of a single endochronic unit was the main reason why better fits of the data could not be achieved by Cuellar et al. (14) for both small and large strain amplitudes. An analogy with viscoelasticity is helpful to understand why this occurs; Z_1 and Z_2 may be regarded as relaxation times in the sense of ξ (rather than t), and experience with viscoelasticity teaches us that the number of relaxation times must be increased when a broader range of times is considered. Aside from this argument, the coupling of two parallel units causes the unloading stress-strain diagram to start more steeply and to be more curved, and this is needed to improve the data fits. Note also that the use of two parallel endochronic units is analogous to the "overlay" model used by several investigators (e.g. Zienkiewicz, (33)) in classical viscoplasticity.

Hysteresis and Jump-Kinematic Hardening

The hysteresis in cyclic loading is controlled by $\alpha_{ij}^{(1)}$, $\alpha_{ij}^{(2)}$, and c, and these must now be determined. For monotonic loading, the response curves can be easily modeled without these parameters, and so we may set $c = 1$ and $\alpha_{ij}^{(1)} = \alpha_{ij}^{(2)} = 0$ for this case. The question which remains is how these parameters should vary with unloading and reloading. The basic objective to be satisfied is the closing of the hysteresis loops during an unload-reload cycle in which the initial stress, σ_o, is reduced to $\sigma_o - S$ and subsequently again increased back to σ_o. With the original endochronic theory, the hysteresis loops during which the stress does not change sign do not close if their amplitude S is smaller than a certain critical value, τ_o; this means that the work, ΔW, done on the material during the cycle is negative. Moreover, when unloading reverses to reloading, the slope of the stress-strain curve becomes smaller, while all test data indicate that it should become higher. Valanis (30) recently tried to remedy this problem without introducing inequality conditions; he redefined the intrinsic time by replacing $d\xi$ with an expression which depends on both de_{ij} and ds_{ij}. However, this appears to mitigate the problem only partly since for a sufficiently small S, compared to τ_o, the hysteresis loops still do not close and the slope does not become steeper as unloading reverses to reloading.

Elimination of this problem for arbitrarily small values of S while simultaneously allowing for inelastic unloading and reloading behavior

can be achieved by introducing certain inequality conditions in a method called jump-kinematic hardening (4). At the time when loading changes to unloading, the center of the yield surface, $\alpha_{ij}^{(1)}$ and $\alpha_{ij}^{(2)}$, is considered to jump to the upper extreme stress point, $s_{ij}^{(1)}$ and $s_{ij}^{(2)}$ (point 1 in Fig. 1(*c*)), and then again to the lower extreme stress point (point 2 in Fig. 1(*c*)) when unloading changes to reloading. At the same time, the rate of accumulation of the intrinsic time is considered to change, which is indicated by the cyclic parameter, c, in Eq. 3; for the first or virgin loading, $c = 1$, while for unloading $c = c_u$, and for reloading $c = c_r$, where $c_u < 1$ and $c_r < 1$.

Between the loading reversals we keep $\alpha_{ij}^{(1)}$ and $\alpha_{ij}^{(2)}$ constant, chiefly because it does not seem necessary to vary these gradually in order to fit the test data well. However, a gradual variation of $\alpha_{ij}^{(1)}$ and $\alpha_{ij}^{(2)}$ could be incorporated as well, to represent the development of stress-induced anisotropy. To reflect the anisotropy due to preconsolidation, one could also use nonzero $\alpha_{ij}^{(2)}$ at the outset.

The condition of non-negative energy dissipation during the unload-reload cycle imposes a certain restriction on c_u and c_r. This has been determined previously (4) and will be reviewed here only briefly. Consider the simple shear stress $\tau = s_{12}$ and strain $\gamma = 2e_{12}$, in which case $d\xi = [(de_{12}de_{12} + de_{21}de_{21})/2]^{1/2} = |d\gamma|/2$, and let attention be limited to a single endochronic unit. Then, the stress-strain relation, Eq. 2, has the form $d\tau = Gd\gamma - d\tau''$ where $d\tau'' = (\tau - \alpha)\, cF|d\gamma|/(2Z)$ and $\alpha = \alpha_{12}^{(1)}$. If the unloading decrement, $d\gamma$, is followed by an equal reloading increment, $d\gamma$, the elastic increment, $Gd\gamma$, retains its magnitude and changes its sign, whereas the inelastic stress increment, $d\sigma''$, keeps the same sign if $\tau - \alpha$ remains of the same sign; the reloading slope is therefore always less than the unloading slope (Fig. 1(*b*)) (this also implies that $\Delta\pi$, Eq. 12, is negative during unloading). Evidently, $\tau - \alpha$ must change sign, and this can only be achieved by the jump in α, as just described. Defining $|\tau - \alpha| = \bar{\tau}$ and $|\gamma - \gamma_o| = \bar{\gamma}$, where γ_o is the value of γ at the last extreme point, we may now write

$$d\bar{\tau} = Gd\bar{\gamma} - \bar{\tau}\frac{c}{2}F\, d\bar{\gamma} \quad \ldots\ldots (6)$$

for either unloading or reloading, with the initial condition that $\bar{\tau} = 0$ at $\bar{\gamma} = 0$. If amplitude S is small, F and G may be considered constant, and Eq. 6 may then be easily integrated. We have $d\bar{\tau} = G(a - a\bar{\tau})\, d\bar{\gamma}$, where $a = cF/2G$, and this is approximately equivalent to $d\bar{\gamma} = (1 + a\bar{\tau})\, d\bar{\tau}/G$. The work of the stress, $\bar{\tau}$, is defined as $\bar{W} = \int \bar{\tau} d\bar{\gamma}$ and is obtained by integrating $d\bar{W} = (1 + a\bar{\tau})\, \bar{\tau} d\tau/G$. Integrating also the expressions for $d\bar{\gamma}$ and $d\bar{\tau}$, we obtain

$$\bar{\gamma} = \frac{\bar{\tau}}{G}\left(1 + \frac{a}{2}\bar{\tau}\right); \quad \bar{W} = \frac{\bar{\tau}^2}{2G}\left(1 + \frac{2a}{3}\bar{\tau}\right) \quad \ldots\ldots (7)$$

Substituting $\bar{\tau} = S$, we get the integral from one extreme stress point to the next. The net change, $\Delta\gamma$, of γ over the unload-reload cycle and the dissipated work, ΔW, may now be calculated. The value of $\Delta\gamma$ follows by subtracting $\bar{\gamma}$ for $c = c_u$ from $\bar{\gamma}$ for $c = c_r$, both for $\bar{\tau} = S$ (Eq. 7), and ΔW may be calculated as $\Delta W = \Delta W_1 - \Delta W_2$, where ΔW_1 and ΔW_2 are

the cross-hatched areas in Fig. 1(*c*). In this sense the condition $\Delta W \geq 0$ represents Drucker's stability postulate. It is easy to check that ΔW equals area 1241 minus area 24352 plus 2352 (Fig. 1(*c*)), where area 24352 equals $S\gamma_1$ (where γ_1 is the value of $\bar{\gamma}$ for $c = c_r$ and $\bar{\tau} = S$) and areas 1241 and 2352 are obtained from Eq. 7 as $\bar{W}$ for $c = c_u$ and $c = c_r$ with $\bar{\tau} = S$. In this manner we obtain

$$\Delta\gamma = \frac{F}{2G}(c_r - c_u)S^2; \quad \frac{\Delta W}{W_1} = \frac{2}{3}F\left(c_u - \frac{c_r}{2}\right)S \quad \ldots\ldots\ldots\ldots\ldots\ldots\ldots\ldots (8)$$

in which $W_1 = S^2/G$. To obtain cyclic strain accumulation for asymmetric stress cycling, we must have $\Delta\gamma > 0$, and to obtain non-negative energy dissipation, we must have $\Delta W \geq 0$; these conditions provide the final result:

$$c_u < c_r \leq 2c_u \quad \ldots\ldots\ldots\ldots\ldots\ldots\ldots\ldots\ldots\ldots\ldots\ldots\ldots\ldots\ldots\ldots\ldots\ldots\ldots\ldots (9)$$

which has been obtained in a more general form by Bažant (4). The values $c_u = 0.40$ and $c_r = 0.45$ were used for all data fitting shown herein.

Now, the unloading and reloading criteria must be defined in an invariant way. It does not seem suitable to define them in terms of stress, because dense sand can exhibit strain softening (stress reduction with increasing strain), in which case the stress decreases both for loading ($d\gamma \geq 0$) and for unloading ($d\gamma < 0$). Proper distinction can be made either in terms of a strain criterion or in terms of work, of which the latter seems more reasonable because it is more closely related to the choice of the loading function, Φ. Since the inelastic strain is caused predominantly by deviatoric straining it seems to be an acceptable approximation to include under W only the deviatoric part.

$$W = \int s_{km}\,de_{km} \quad \ldots\ldots\ldots\ldots\ldots\ldots\ldots\ldots\ldots\ldots\ldots\ldots\ldots\ldots\ldots\ldots\ldots\ldots\ldots\ldots (10)$$

and define the loading-unloading-reloading criteria as follows:

1. for $dW \geq 0$ and $W = W_o$; $c = 1$ (virgin loading)..... (11*a*)
2. for $dW < 0$; $c = c_u$ (unloading)..... (11*b*)
3. for $dW \geq 0$ and $W < W_o$; $c = c_r$ (reloading)..... (11*c*)

in which W_o denotes the maximum value of W attained up to the current time. According to Eqs. 11, the regimes for symmetric cycling typically change, as indicated in Fig. 1(*d*).

The foregoing criteria are suitable for defining c_u and c_r, but if they were also applied to determine the extreme points where $\alpha_{ij}^{(1)}$ and $\alpha_{ij}^{(2)}$ are set equal to $s_{ij}^{(1)}$ and $s_{ij}^{(2)}$, the hysteresis loops would look as shown in Fig. 1(*e*) (exaggerated). The abrupt changes of slope do not appear too realistic; rather, it is preferred that both the downward branch and the upward branch have a continuous slope. This may be achieved by using the following second-order work quantity as an unloading-reloading criterion for $\alpha_{ij}^{(1)}$ and $\alpha_{ij}^{(2)}$

$$\Delta\pi = ds''_{km}\,de_{km} = \left[(s_{ij}^{(1)} - \alpha_{ij}^{(1)})\frac{d\zeta}{Z_1} + (s_{ij}^{(2)} - \alpha_{ij}^{(2)})\frac{d\zeta}{Z_2}\right] de_{km} \quad \ldots\ldots\ldots\ldots (12)$$

in which ds''_{km} is the inelastic stress decrement. According to Il'yushin's stability postulate (15), $\Delta\pi$ is always non-negative when the inelastic stress increment is non-zero. In step-by-step calculation, $\Delta\pi$ is negative during the step in which loading changes to unloading or vice versa (this is because of the one-step lag between the strain increment and the stress increment). Thus, when $\Delta\pi < 0$, we set $\alpha_{ij}^{(1)} = s_{ij}^{(1)}$ and $\alpha_{ij}^{(2)} = s_{ij}^{(2)}$, thereby making $\Delta\pi$ positive for the subsequent loading step. With this criterion for determining $\alpha_{ij}^{(1)}$ and $\alpha_{ij}^{(2)}$, the hysteresis loops are smooth, as pictured in Fig. 1(*d*).

To complete the rules for loading regimes, we must consider ξ throughout the transition from reloading to virgin loading. Although test data for sand are lacking in this case, analogy with other materials indicates that, with a continuous accumulation of ξ, the response for virgin loading after a number of unload-reload cycles would overshoot the virgin loading curve (Fig. 1(*f*)), which would be incorrect. This overshoot may be prevented by setting $\xi = \xi_o$ at the point where reloading changes to virgin loading (Eqs. 11*b* and 11*c*); ξ_o denotes the value of ξ when virgin loading last changed to unloading.

It should be also mentioned that a further improvement of the jump-kinematic hardening rule has recently been made (and implemented in a large computer code) by J. Jeter (18). He proposed to relocate the center of the loading surface when reloading changes to virgin loading after many previous stress cycles at intermediate stress levels.

The version of endochronic theory that satisfies the foregoing restricton of non-negative work dissipated by hysteresis loops may be called hysteretic.

Elastic Moduli

For the two-unit model (Fig. 1(*a*)), the shear modulus is given by $G = G_1 + G_2$, and the shear moduli for individual units have been considered in calculations as $G_1 = 0.6\,G$ and $G_2 = 0.4G$. The combined shear modulus G must depend on both hydrostatic stress, $p = -\sigma$, and void ratio, e. This has been considered in previous studies (14,10), except that relative density, D_r, was used instead of e (D_r has a negligible influence on the shear wave velocity; p. 153 of Ref. 20). The use of void ratio is preferred in this study because the definition of D_r is subject to significant variations in test procedures and interpretation. Moreover, G was considered to be a function of the maximum value of the deviator strain invariant attained up to the current time. This last dependence, however, appears to be unnecessary when the two-unit model is considered. The selected function,

$$G = 90\frac{(2.97 - e)^2}{1 + e}\sqrt{-I_1}; \quad I_1 = \sigma_{kk} \quad \ldots\ldots\ldots\ldots\ldots\ldots\ldots\ldots\ldots\ldots\ldots\ldots\ldots\ldots (13)$$

in which G and I_1 are in psi (psi = 6,895 N/mm^2). Equation 13 is similar in form to that used by Richart et al. (21) for the shear modulus. The void ratio is considered to remain constant at its initial value, because the changes in e caused by usual deformation histories (e.g., in seismic loading before liquefaction) are minor compared to the range of e encountered in various sand deposits. Assuming that the elastic properties

do not exhibit stress-induced anisotropy, it suffices to describe the elastic behavior by G and K; hence, the bulk modulus, K, can be expressed as

$$K = \frac{2G(1+\nu)}{3(1-2\nu)} \quad (14)$$

in which $\nu = 1/3$ was used in fitting test data. For many sands, though, values between $\nu = 0.1$ and 0.15 may be more appropriate.

Hardening-Softening Function

The path length ξ may be, in a physical sense, regarded as a rearrangement measure, characterizing the degree of rearrangement of sand grain configurations (3,14). The function F in Eq. 3, called the hardening-softening function, introduces the various contributions of $d\xi$ to inelastic strain, depending on other state parameters. The description of hardening and softening of inelastic response by means of changes in the rate of accumulation of intrinsic time is the most useful practical feature of endochronic theory. It makes hardening and softening easily controlled and understood. Hardening and softening are defined by the function F, which is considered basically in the form

$$F = \frac{1 + J_2 f(\bar{\gamma}) D(e)}{1 + J_2 g(I_1)} h(\xi) \quad (15)$$

where $\bar{\gamma} = (e_{km}e_{km}/2)^{1/2}$ is the strain intensity (a strain invariant) and I_1 is the first stress invariant. The detailed forms of these functions are given in the Appendix.

The function $g(I_1)$ increases with $(-I_1)$ and models the fact that the response of sand becomes stiffer as the hydrostic pressure increases. The function $f(\bar{\gamma})$ models the fact that, at large shear strain, the material becomes softer (which is explained by loss of contact between some grains). The function $D(e)$, which decreases as e increases models the fact that a softer response is associated with a larger void ratio.

Based on numerical calculation using endochronic theory, the lateral stress in the simple shear test increases very rapidly as the deformation begins. Since the first maximum stress state it is essentially equal to the vertical stress (i.e., the stress state is essentially hydrostatic and $J_2 \approx \tau^2$, where $\tau = s_{12}$ is the applied shear stress). This behavior has been also observed experimentally (20). In cyclic simple shear tests, the maximum value of τ^2 within a given cycle is generally much smaller than the maximum value of J_2 that is induced in triaxial tests (where $J_2 = (\sigma_1 - \sigma_3)^2/3$, σ_1 and σ_3 being the axial and lateral principal stresses, respectively). Therefore, the magnitude of J_2 provides, in terms of stress invariants, a useful distinction between the simple shear test and the triaxial test. Hence, if the fitting of data from each of these tests requires the use of different functions F, as it invariably will, the different terms should be made to vanish as J_2 vanishes. This simple observation has been utilized successfully to simultaneously fit test results from each of these two types of test with the same constitutive relation. Another marked difference between the two tests is the fact that the mean of the shear strain, $\bar{\gamma}$, over the cycle increases in the triaxial test but not in the simple shear

test; however, there seems to be no need to exploit this difference in the invariants.

The function $h(\xi)$ must decrease as ξ increases in order to model the hardening that takes place—primarily the contraction and the steepening of the hysteresis loops as the number of load cycles increases. This is because ξ is essentially proportional to the number of cycles. Note that Eq. 15 is chosen in a form which gives $F = h(\xi)$ for $J_2 = 0$. This is approximately the case for simple shear test because in these tests there appears to be no need for hardening or softening as a function of $\bar{\gamma}$, I_1, or e. Of course, I_1 and e still affect the stiffness in cyclic shear tests indirectly by means of G (Eq. 13).

Densification and Dilatancy

The densification due to cyclic shear strains has been successfully modeled with endochronic theory (Bažant and Krizek, 10; Cuellar et al., 14), and therefore the original form has been essentially retained. The change of volume due to densification is described by a function of the form

$$d\lambda_1 = -\frac{f_1(\bar{\gamma}) g_1(I_1)}{h_1(\xi)} k_1(J_2^{\alpha}) D_1(e) d\xi \quad (16)$$

in which $J_2^{\alpha} = \alpha_{km}\alpha_{km}/2$ and invariant J_2^{α} has the useful properties that it is zero if we choose, as we did, $\alpha_{ij} = 0$ for the first monotonic loading, and is essentially constant after the first stress maximum for a given shear stress amplitude in the simple cyclic shear tests. Thus, the function $k_1(J_2^{\alpha})$ may be used to distinguish the behavior for virgin (monotonic) loading and for subsequent cyclic loading. As in the previous studies (10,14), $d\lambda_1$ is taken proportional to $d\xi$, because ξ measures the grain rearrangments, which is the source of densification.

The function $D_1(e)$ must increase with an increase in the void ratio, e, in order to properly model the stronger tendency of a looser sand to densify. The functions f_1, g, and h_1 are essentially the same as in the previous work (1) and Cuellar et al. (14). The function f_1 increases with $\bar{\gamma}$ to depict the increase in the densification rate (per unit path length of ξ) as the strain amplitude increases ($\bar{\gamma}^2 = J_2^{\varepsilon} = e_{km}e_{km}/2$). The function $g_1(I_1)$ increases with hydrostatic pressure, $p = -I_1/3 = -\sigma$, and the function $h_1(\xi)$ increases with ξ to reflect the reduction in the densification rate with an increasing number of cycles.

In addition to densification, the shearing of sand can also induce dilatancy, designated by λ_2. This phenomenon, which is much less important than densification and was neglected in the previous work (10,14), is sometimes observed at the beginning of virgin (monotonic) shear deformation; it is due to the fact that sand grains must first slide over each other before they can find and fill some empty intergranular spaces, thereby rearranging themselves to form denser grain configurations. The expressions for $d\lambda_2$ must be constructed so that its effect is very small within the strain range of cyclic simple shear tests; this is because the dilatancy is usually observed only in triaxial tests with small confining pressure. Therefore, $d\lambda_2$ must increase sharply with $\bar{\gamma}$, which is given

by the function $f_2(\tilde{\gamma})$. The expression for $d\lambda_2$ is chosen in the form

$$d\lambda_2 = \frac{f_2(\tilde{\gamma})\, D_2(e)}{g_2(I_1)\, h_2(\xi)}\, d\xi \qquad (17)$$

As in case of densification, $d\lambda_2$ is assumed to be proportional to $d\xi$, because the source of dilatancy is the same. The function $g_2(I_1)$ increases mildly with hydrostatic pressure, $p = -I_1/3$, because $d\lambda_2$ is found to be somewhat smaller at higher pressures (apparently the result of increased friction that impedes grain rearrangments). The function $h_2(\xi)$ increases

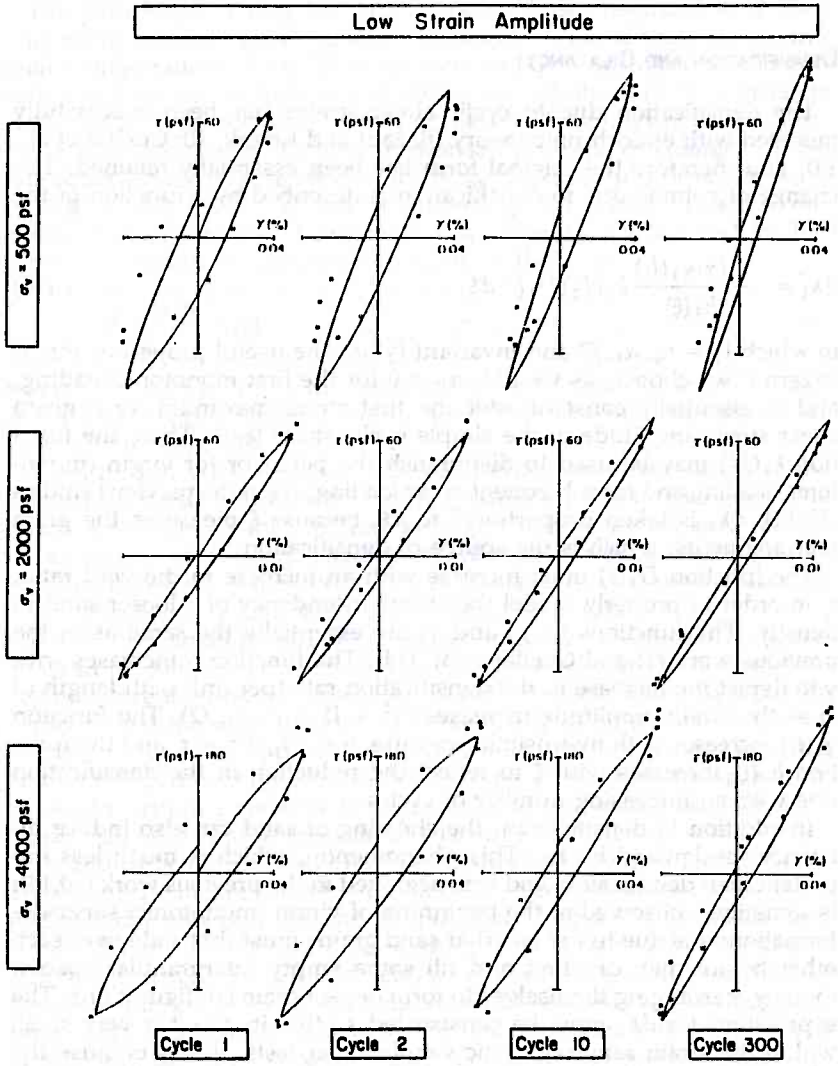

FIG. 2.—Test Data Points from Cyclic Simple Shear Tests by Silver and

very strongly with ξ, so as to make $d\lambda_2$ virtually vanish for subsequent cycles, as well as for the larger strains in the first cycle. The function $D_2(e)$ decreases with an increase in the void ratio (this is opposite to $D_1(e)$), and it is needed to reflect the fact that a looser sand has a smaller tendency for dilatancy but a higher tendency for densification.

By including both densification and dilatancy terms, it has been possible to model quite realistically the volume changes in both cyclic simple shear tests and triaxial tests with the same constitutive relation. The total volumetric deformation is expressed as

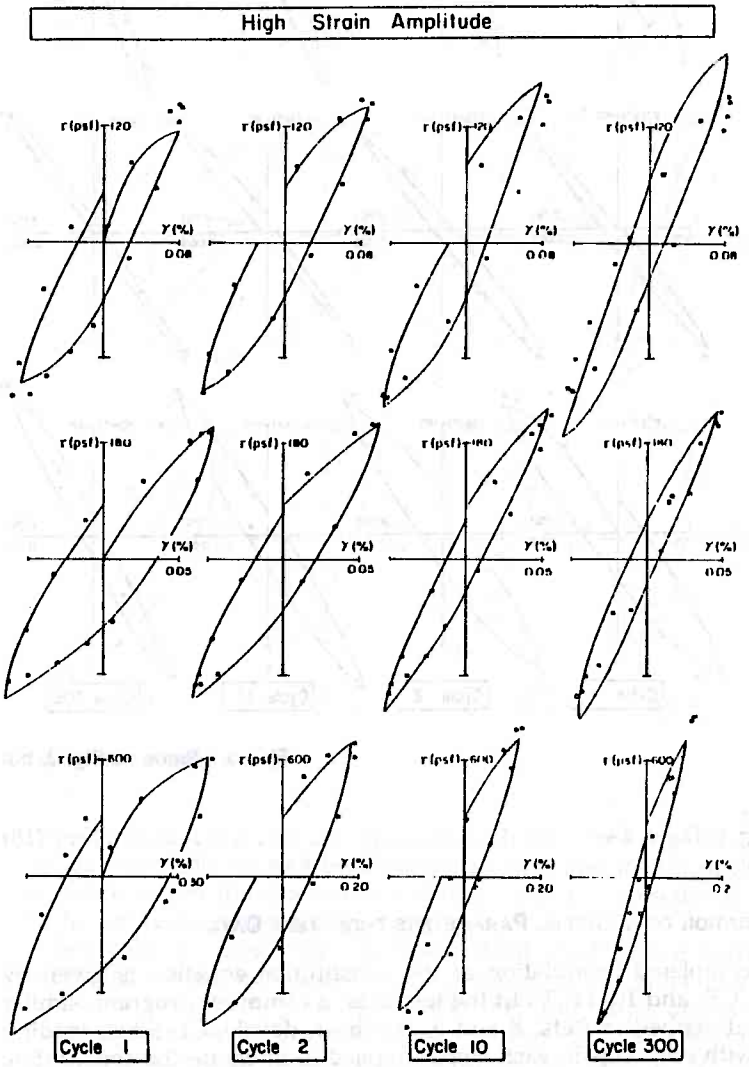

Seed (1971) for Relative Density 45%, and Fits by the Present Theory

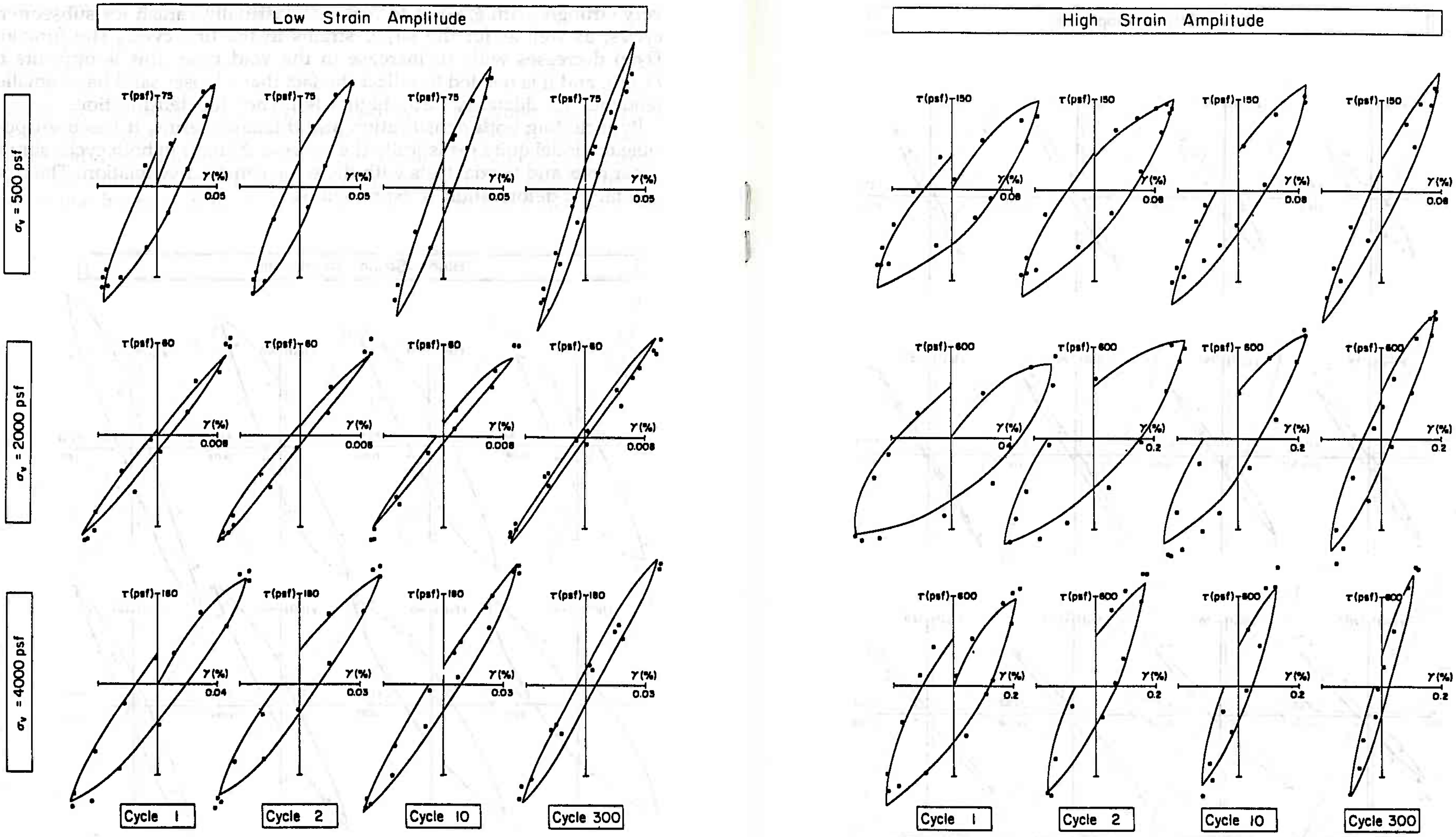

FIG. 3.—Same as Fig. 2, but for Relative Density 60%

$$d\epsilon = \frac{d\sigma}{3K} + d\lambda_1 + d\lambda_2 \quad \text{(18)}$$

Identification of Material Parameters from Test Data

The completed formulation of the constitutive equation is given by Eqs. 1, 3, 5, and 10–18. To fit the test data, a computer program, similar to that described in Refs. 8 and 9, has been developed. Small loading steps, with iterations in each step, are used to integrate the constitutive relation numerically for: (1) Specified forms of material functions; (2) given material parameters; and (3) prescribed boundary conditions of the test

to be simulated (e.g., simple shear, triaxial, etc.). The response diagrams are automatically plotted by Calcomp plotter, and a sum of the square deviations from the characteristic data points (the objective function to be minimized) is evaluated.

Test data obtained from Silver and Seed (26,27) have been used to determine the material functions and parameters (see Appendix I). These data have been fitted quite closely over their full range, and several typical fits of hysteresis loops are shown in Figs. 2, 3, and 4. Ranges are: (1) 1 to 300 load cycles (four of the hysteresis loops indicated for 300 load cycles were actually obtained for a lesser number of cycles in order to be consistent with available data); (2) 0.008% to 0.2% shear strain am-

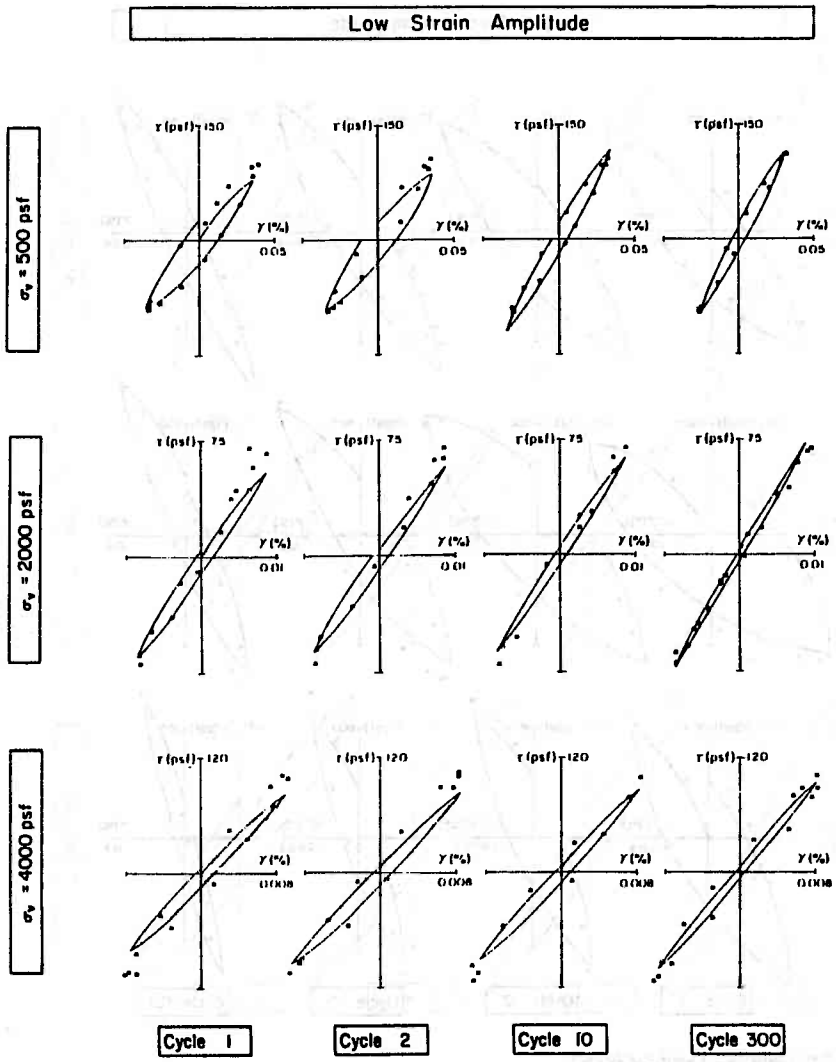

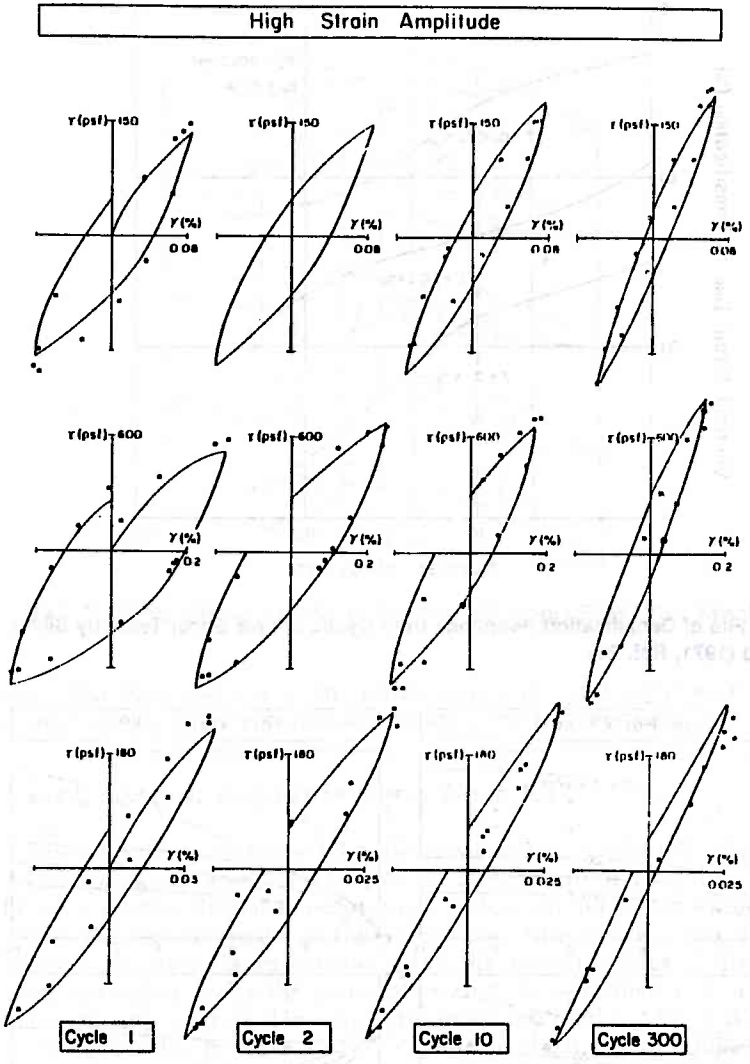

FIG. 4.—Same as Fig. 2, but for Relative Density 80%

plitudes; (3) 45% to 80% relative densities (which correspond to void ratios from 0.83 to 0.71); and (4) 500 psf (24 kPa) to 4,000 psf (192 kPa) vertical stress.

It is noteworthy that the same theory is used to characterize the test data obtained from both cyclic simple shear tests (Fig. 5) and triaxial tests (19) (Fig. 6). The fact that these two different sets of test data have been analyzed on a common basis (a feat often aspired, but never achieved) introduces the possibility of making inferences from one type of test (say triaxial) on the behavior simulated by the other type of test.

In fitting the cyclic simple shear data, the state before shear straining but after the application of a given vertical stress, σ_1, is considered as the initial state of the material. This assumption was necessary because the deformation due to the application of σ_1 was unavailable, although it would certainly be more correct to use the state before the application of σ_1 as the initial state. The lateral stress, σ_3, was assumed equal to 0.5 σ_1 in the initial state. This means that the second invariant of the deviator stress, J_2, exerts a significant effect on the initial state. The initial deviator stresses, s_{11}, s_{22}, and s_{33}, due to σ_1 are assumed to be distributed over the two parallel endochronic Maxwell units (Fig. 1(*a*)) in proportion to G_1 and G_2. The densification is measured as an increase from

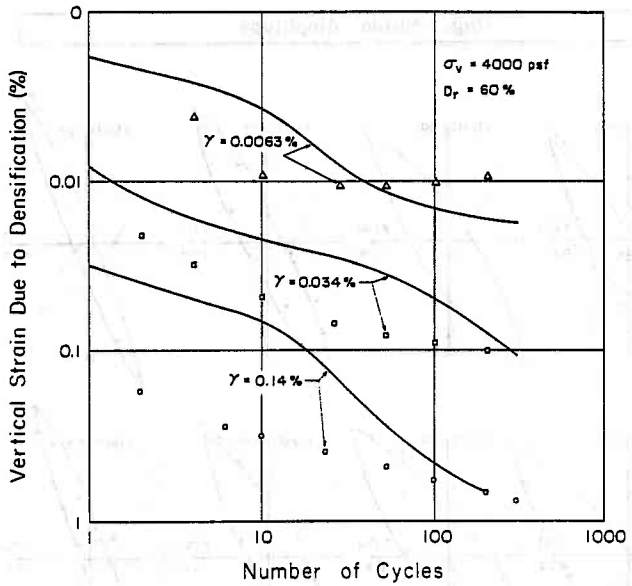

FIG. 5.—Fits of Densification Response from Cyclic Simple Shear Tests by Silver and Seed (1971, Ref. 26)

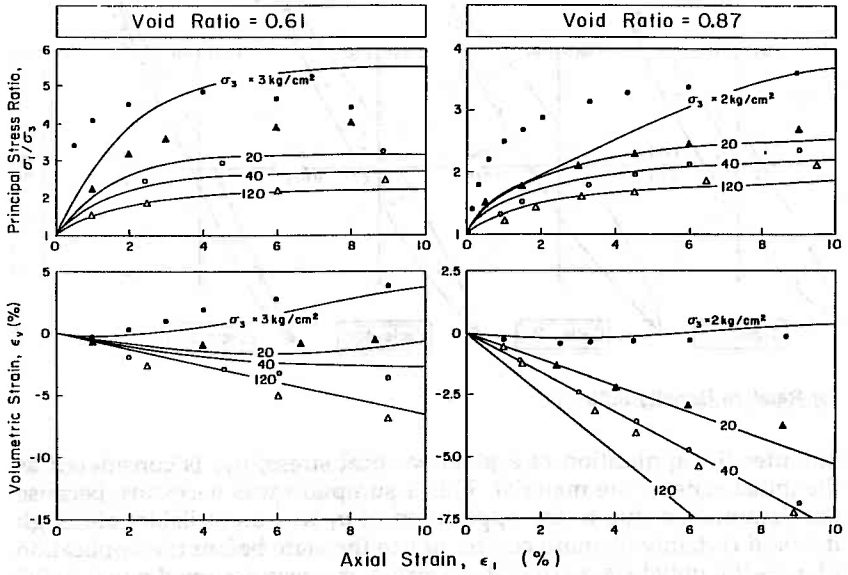

FIG. 6.—Fits of Densification Response from Triaxial Tests by Lee and Seed (1967)

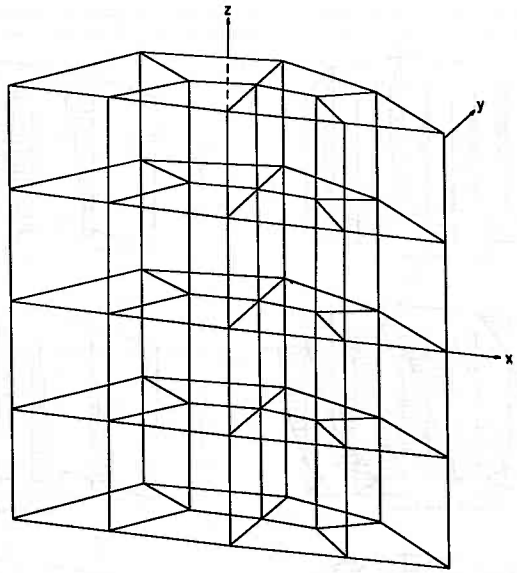

FIG. 7.—Finite Element Mode for One Half of Simple Shear Test Specimen

the initial state under a given vertical stress, σ_1, and not from the state of zero stress, for which measurements were not reported.

Three-Dimensional Analysis of Simple Shear Test

One commonly employed simple shear test is conducted on a cylindrical specimen which is enclosed in a wire-reinforced rubber membrane; a relative displacement normal to the cylinder axis is induced between the circular ends of the specimen while keeping the distance between the end planes constant. The fits shown in Figs. 2 through 5 were calculated under the assumption that the specimen is in a homogeneous state of stress. However, this oversimplified condition is known to be unrealistic, because a state of uniform shear stress would require the application of shear stresses at the cylindrical surface of the specimen, which is not actually done. The question therefore, becomes one of evaluating the importance of this erroneous assumption in the interpretation of test data.

One attempt to answer this question has been based on the assumption of linear elastic behavior for the sand. However, since the material is highly nonlinear, a linear elastic analysis is of questionable value. Therefore, a three-dimensional finite element analysis of the simple shear test has been undertaken herein by use of endochronic theory. Because this work was carried out before completing the development of the present constitutive relation, the original endochronic theory for sand (10,14) was used for this finite element analysis.

All finite elements were eight-node hexahedral isoparametric elements

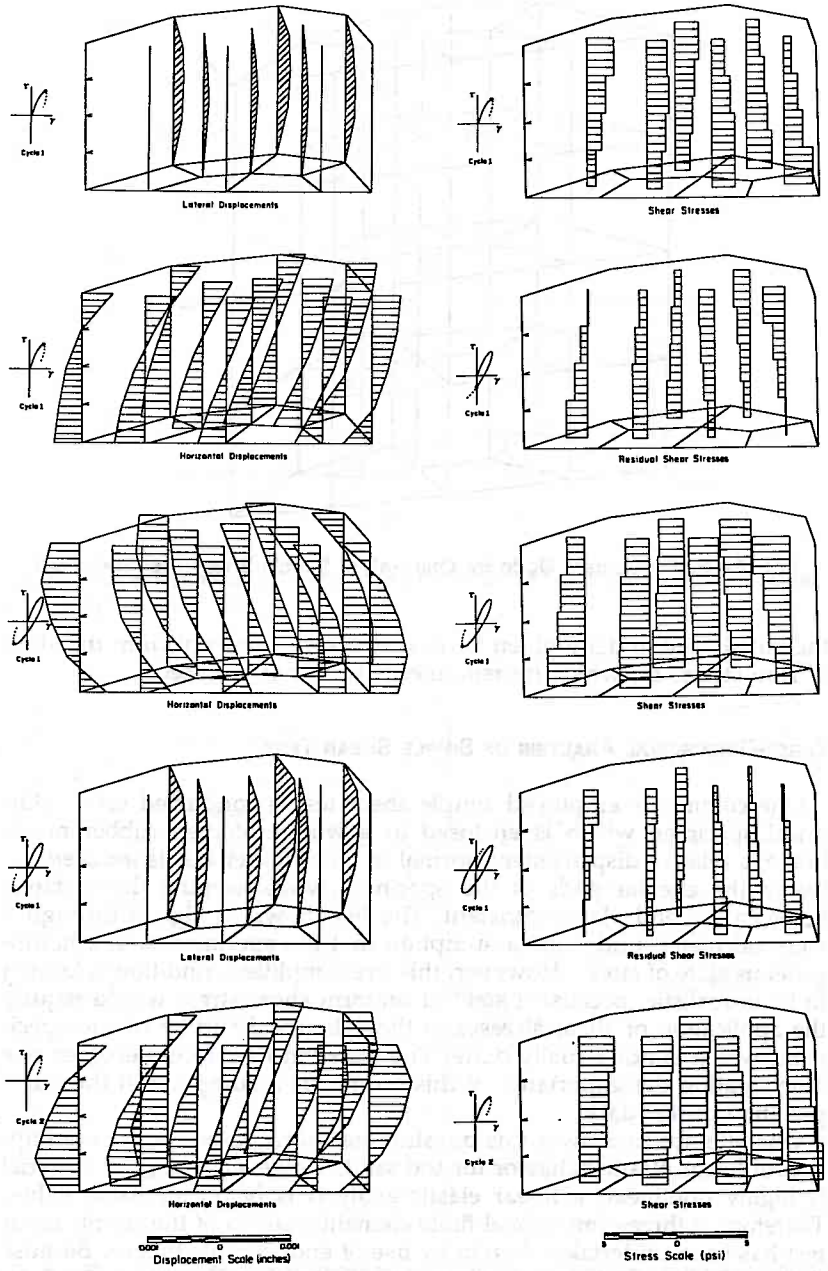

FIG. 8.—Distributions of Displacements and Stresses in Cyclic Shear Test Specimen

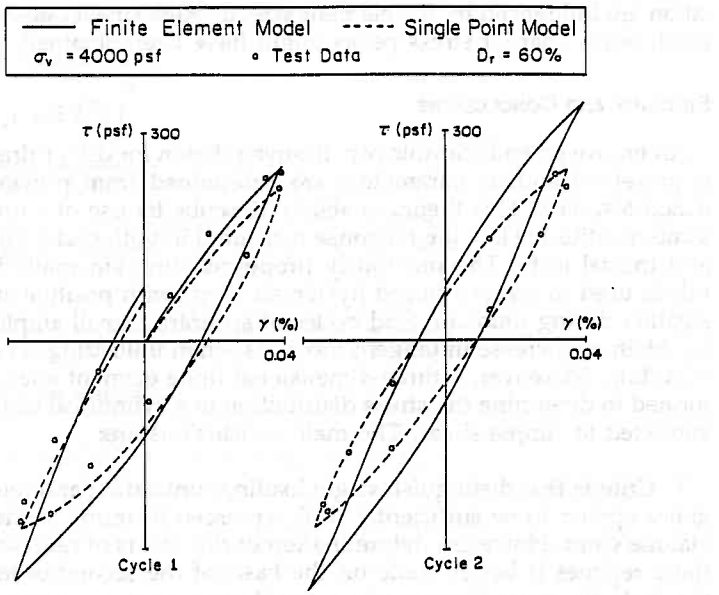

FIG. 9.—Comparison of Hysteresis Loops Determined from Finite Element Model and Single Point Model

(denoted as ZIB-8 by Zienkiewicz, 34) with two integration points in each direction. However, the strain and stress were evaluated only at the centroid. Since the sand specimen is assumed to be bonded to the end plates, a uniform horizontal displacement was imposed on the top and bottom faces in opposite directions. The reinforcing wires in the surrounding (otherwise flexible) membrane were modeled by straight bar elements connecting the surface nodes; these elements had the same stiffness as the wires. The specimen was subdivided into 48 elements (Fig. 7 shows one-half of the specimen), but due to the symmetry and the antisymmetry of the shear deformation, only one quarter of the specimen (12 elements with 42 degrees of freedom) was analyzed. The boundary conditions on the plane xz were those of symmetry ($u_y = \sigma_y = \tau_{xz} = \tau_{yz} = 0$), and the boundary conditions on the plane xy expressed the fact that in any pair of nodes located symmetrically against axis y the nodal forces of y direction from the element must be the same and those of x and z directions must be of equal magnitude and opposite sign.

Typical displacement and stress distributions obtained by the finite element endochronic analysis are illustrated in Fig. 8. Although Fig. 9 shows that the hysteresis loops generated by this sophisticated analysis do not differ much from those that result from the assumption of uniform stress, the stresses are quite nonuniform, with the minimum and maximum stresses differing by as much as 200%. Also, note that significant residual stresses remain upon unloading. It should also be realized that the peak stress values obtained in the finite element calcu-

lation are influenced by the element size; if much smaller elements were used, much sharper stress peaks might have been obtained.

Summary and Conclusions

An improved endochronic constitutive relation for dry or drained sand is presented and its parameters are determined from previously published test data. This theory is able to describe by use of a one and the same constitutive law the response measured in both cyclic simple shear and triaxial tests. The previously proposed jump-kinematic hardening rule is used to achieve closed hysteresis loops with positive energy dissipation during unload-reload cycles of arbitrarily small amplitude, and to obtain an increase in tangent modulus when unloading is reversed to reloading. Moreover, a three-dimensional finite element analysis is performed to determine the stress distribution in a cylindrical test specimen subjected to simple shear. The main conclusions are:

1. Criteria that distinguish virgin loading, unloading and reloading regimes appear to be sufficiently well expressed in terms of the total deviatoric work. However, determination of the points of reversal between these regimes is better made on the basis of the second-order work of the inelastic stress increment on the deviatoric strain increment. Furthermore, at the point of transition from reloading to virgin loading, the intrinsic time must be reset to its last previous value at virgin loading.
2. Two endochronic units coupled in parallel make it possible to achieve good agreement with test data over a broad range of strain magnitude and to obtain proper curvature of the unloading stress-strain diagrams.
3. The inelastic volume change in the model includes both densification (as in the previously published formulation) and dilatancy (which occurs when a dense sand is sheared). Both dilatancy and densification appear to be proportional to the deviatoric path length (rearrangement measure).
4. Coefficients for the dependence of densification and dilatancy function (Eq. 16), of the partial elastic moduli of the two parallel endochronic units, and of the hardening-softening function (Eq. 15) upon the stress and strain invariants and the intrinsic time are identified and rules for their changes in loading-unloading-reloading transitions are determined. Furthermore, certain material properties are determined as functions of the void ratio.
5. The resulting endochronic model has a considerably broader applicability than the original endochronic model for sand (14).
6. A three-dimensional finite element analysis of the simple shear test with endochronic theory reveals significant stress nonuniformity and residual stresses in the specimen; however, the hysteresis loops obtained by this sophisticated analysis are not very different from those calculated under the assumption of uniform stress.

Acknowledgment

The support provided during 1977–79 under National Science Foundation Grant No. ENG-787777 is gratefully acknowledged.

Appendix I.—Material Characterization

Material Functions.—

$$F = \frac{1 + a_o J_o \sqrt{\bar{\gamma}} \left(\frac{a_2}{e}\right)^2}{1 + J_o(a_3 + |a_4 I_1|^{0.4})} \frac{1 + a_5 \xi}{1 + \beta_1 \xi + \beta_2 \xi^2}; \quad J_o = \frac{J_2}{a_1 + J_2}$$

$$d\lambda_1 = -e^3 |c_6 I_1^a|^{3/4} \frac{(1 + c_7 J_2^a)\, \gamma'' \gamma^{2/3}}{1 + c_9 \xi + c_{10} \xi^2} d\xi; \quad \gamma'' = \left(\frac{2\bar{\gamma}}{c_8 + \bar{\gamma}}\right)^2$$

$$d\lambda_2 = \frac{c_1}{e^3} \frac{\gamma'}{1 + |c_2 I_1|^{0.4}} \frac{d\xi}{1 + c_4 \xi + c_5 \xi^2}; \quad \gamma' = \left(\frac{2\bar{\gamma}}{c_3 + \bar{\gamma}}\right)^2 \quad \text{..... (19)}$$

Material Parameters.—

$$a_o = 1.2; \quad a_1 = 4\left(\frac{\text{kp}}{\text{cm}^2}\right)^2; \quad a_2 = 0.61; \quad a_3 = 1.8;$$

$$a_4 = 0.686 \frac{\text{cm}^2}{\text{kp}}, \quad a_5 = 200, \quad c_1 = 0.823, \quad c_2 = 474 \frac{\text{cm}^2}{\text{kp}}, \quad c_3 = 0.05,$$

$$c_4 = 2, \quad c_5 = 200, \quad c_6 = 0.041 \frac{\text{cm}^2}{\text{kp}}, \quad c_7 = 25\left(\frac{\text{cm}^2}{\text{kp}}\right)^2,$$

$$c_8 = 0.0002, \quad c_9 = 10, \quad c_{10} = 600, \quad \beta_1 = 500, \quad \beta_2 = 660 \quad \text{..... (20)}$$

in which $\text{kp/cm}^2 = 0.987\ \text{N/mm}^2 = 14.22$ psi.

Appendix II.—Relation to Some Other Recent Studies

Another way of achieving positive energy dissipation in arbitrary stress cycles was recently reported by Valanis (34) and further developed by Valanis and Read (32). Two features are essential to their formulation: (1) Definition of intrinsic time as the length of the path of inelastic strains de_{ij}^{pl}, rather than the total strains de_{ij} (as in Eq. 3); and (2) the use of history integrals with a kernel that is singular in intrinsic time. Recently, Trangenstein and Read (28) studied for this formulation the tangential stiffness as a function of the angular orientation of the stress increment vector in the stress space, keeping the initial state fixed. Interestingly, the angular dependence that they find is identical to that in classical plasticity based on the normality rule. In particular, they found that the strain response is purely elastic for all stress increment vectors whose projection on the radial vector of current stress state in the deviatoric stress state is non-positive. Thus, it transpires that in this version of the endochronic theory the dependence of incremental stiffness on the stress increment direction is equivalent to the use of classical plasticity; the only difference consists in the scalar dependence of an incremental stiffness parameter on the previous stress and strain history. This, in the writers' opinion, deprives the endochronic theory of one important advantage, namely the possibility to model the behavior in which the response to stress increment vectors that are normal to the radial direction is not elastic but softer than elastic.

APPENDIX III.—REFERENCES

1. Ansal, A. M., Bažant, Z. P., Krizek, R. J., "Viscoplasticity of Normally Consolidated Clays," *Journal of the Geotechnical Engineering Division*, ASCE, Vol. 105, No. GT4, 1979, pp. 519–537.
2. Ansal, A. M., Krizek, R. J., Bažant, Z. P., "Seismic Analysis of an Earth Dam Band on Endochronic Theory," R. Dungar, et al., eds., *Proceedings*, International Symposium on "Numerical Methods in Geomechanics," Zurich, Switzerland, Sept., 1982, published by A. A. Bulkema, Rotterdam, Holland, pp. 559–576.
3. Bažant, Z. P., "Endochronic Theory for Inelasticity and Failure of Concrete Structures-Addendum," *Structural Engineering Report No. 1976-12/2/59*, to Oak Ridge National Laboratory, by the Department of Civil Engineering, Northwestern University, Evanston, Ill. (available from National Technical Information Service, Springfield, Va.), 1976.
4. Bažant, Z. P., "Endochronic Inelasticity and Incremental Plasticity," *International Journal of Solids and Structures*, Vol. 14, 1978, pp. 691–714.
5. Bažant, Z. P., "Work Inequalities for Plastic-Fracturing Materials," *International Journal of Solids and Structures*, Vol. 16, 1980, pp. 873–901.
6. Bažant, Z. P., Ansal, A. M., Krizek, R. J., "Viscoplasticity of Transversely Isotropic Clays," *Journal of the Engineering Mechanics Division*, ASCE, Vol. 105, No. EM4, 1979, pp. 549–565.
7. Bažant, Z. P., Ansal, A. M., and Krizek, R. J., "Endochronic Models for Soils," in Soil Mechanics—Transient and Cyclic Loads, ed. by G. N. Pande and O. C. Zienkiewicz, J. Wiley & Sons, Inc., London, England, 1982, pp. 419–438.
8. Bažant, Z. P., and Bhat, P. D., "Endochronic Theory of Inelasticity and Failure of Concrete," *Journal of the Engineering Mechanics Division*, ASCE, Vol. 102, No. EM4, Aug., 1976, pp. 701–722.
9. Bažant, Z. P., Bhat, P. D., and Shieh, C. L., "Endochronic Theory for Inelasticity and Failure Analysis of Concrete Structures," *Structural Engineering Report No. 1976-12/259*, to Oak Ridge National Laboratory, by the Department of Civil Engineering, Northwestern University, Evanston, Ill. (available from National Technical Information Service, Springfield, Va.), 1976.
10. Bažant, Z. P., and Krizek, R. J., "Endochronic Constitutive Law for Liquefaction of Sand," *Journal of the Engineering Mechanics Division*, ASCE, Vol. 102, No. EM2, Apr., 1976, pp. 225–238.
11. Bažant, Z. P., Krizek, R. J., and Shieh, C. L., "Hysteretic Endochronic Theory for Sand," *Geotechnical Engineering Report No. 79-4/654h*, Northwestern University, Evanston, Ill., Apr., 1979.
12. Bažant, Z. P., and Shieh, C. L., "Endochronic Model for Nonlinear Triaxial Behavior of Concrete," *Nuclear Engineering and Design*, Vol. 47, 1978, pp. 305–315.
13. Blázquez, R. M., Krizek, R. J., Bažant, Z. P., "Site Factors Controlling Liquefaction," *Journal of the Engineering Mechanics Division*, ASCE, Vol. 106, No. GT7, July, 1980, pp. 785–801.
14. Cuellar, V., Bažant, Z. P., Krizek, R. J., and Silver, M. L., "Densification and Hysteresis of Sand Under Cyclic Shear," *Journal of the Geotechnical Engineering Division*, ASCE, Vol. 103, No. GT5, May, 1977, pp. 399–416.
15. Dougill, J. W., "Some Remarks on Path Independence in the Small in Plasticity," *Quarterly Journal of Applied Mathematics*, Vol. 32, 1975, pp. 233–243.
16. Dungar, R., and Nuh, S., "Endochronic-Critical State Models for Sand," *Journal of the Engineering Mechanics Division*, ASCE, Vol. 106, No. EM5, Oct., 1980, pp. 951–968.
17. Hsieh, B. J., "On the Uniqueness and Stability of Endochronic Theory," *Journal of Applied Mehcanics*, ASME, Vol. 47, Dec., 1980, pp. 748–754.
18. Jeter, J. W., "An Evaluation of Endochronic Concrete Theory," *Report*, New Mexico Engineering Research Institute, Albuquerque, N.M., 1982.
19. Lee, K. L., and Seed, H. B., "Drained Strength Characteristics of Sands," *Journal of Soil Mechanics and Foundations Division*, ASCE, Vol. 93, No. SM6, Nov., 1967, pp. 117–141.
20. Pyke, R. M., "Settlement and Liquefaction of Sands Under Multidirectional Loading," Dissertation presented to the University of California, at Berkeley, Calif., in 1973, in partial fulfillment of the requirements for the Degree of Doctor of Philosophy.
21. Richart, R. E., Hall, J. R., and Woods, R. D., "Vibrations of Soils and Foundations," Prentice-Hall, Inc., Englewood Cliffs, N.J., 1970.
22. Rivlin, R. S., "Some Comments on the Endochronic Theory of Plasticity," *International Journal of Solids and Structures*, Vol. 17, 1981, pp. 321–248.
23. Sandler, I. S., "On the Uniqueness and Stability of Endochronic Theories of Material Behavior," *Journal of Applied Mechanics*, ASME, Series E, Vol. 45, 1978, pp. 263–266.
24. Schapery, R. A., "On a Thermodynamic Constitutive Theory and Its Application to Various Nonlinear Materials," B. A. Boley, ed., *Proceedings*, IUTAM Symposium East Kilbride, Springer, N.Y., June, 1968.
25. Sener, C., "An Endochronic Nonlinear Inelastic Constitutive Law for Cohesionless Soils Subjected to Dynamic Loading," Dissertation presented to Northwestern University, at Evanston, Ill., in Aug., 1979, in partial fulfillment of the requirements for the degree of Doctor of Philosophy.
26. Silver, M. L., and Seed, H. B., "Deformation Characteristics of Sand Under Cyclic Loading," *Journal of the Soil Mechanics and Foundations Division*, ASCE, Vol. 97, No. SM8, Aug., 1971, pp. 1081–1098.
27. Silver, M. L., and Seed, H. B., "Volume Changes in Sands During Cyclic Loadings," *Journal of the Soil Mechanics and Foundations Division*, ASCE, Vol. 97, No. SM9, Sept., 1971, pp. 1171–1182.
28. Trangenstein, J. A., and Read, H. E., "Inelastic Response Characteristics of the New Endochronic Theory with Singular Kernel," *International Journal of Solids and Structures*, Vol. 18, No. 11, 1982, pp. 947–956.
29. Valanis, K. C., "A Theory of Viscoplasticity Without a Yield Surface," *Archiwum Mechaniki Stossowanej*, Vol. 23, 1971, pp. 517–551.
30. Valanis, K. C., "On the Endochronic Foundation of Elastic Perfectly Plastic Solids," *Proceedings*, Society of Engineering Science—Fourteenth Annual Meeting, Lehigh University, Bethlehem, Pa., 1977, pp. 761–763.
31. Valanis, K. C., "Endochronic Theory With Proper Hysteresis Loop Closure Properties," *Topical Report SSR-4182*, Systems Science and Software, LaJolla, Calif., Aug., 1979.
32. Valanis, K. C., and Read, H. E., "A New Endochronic Plasticity Model for Soils," *Report EPRI NP-1388 (Project 810-5)*, Electric Power Research Institute, Palo Alto, Calif., Apr., 1980.
33. Zienkiewicz, O. C., "The Finite Element Method," Third Edition, John Wiley & Sons, London, 1977.